Propping Open The Door To The Deep Southern Ocean: An Update

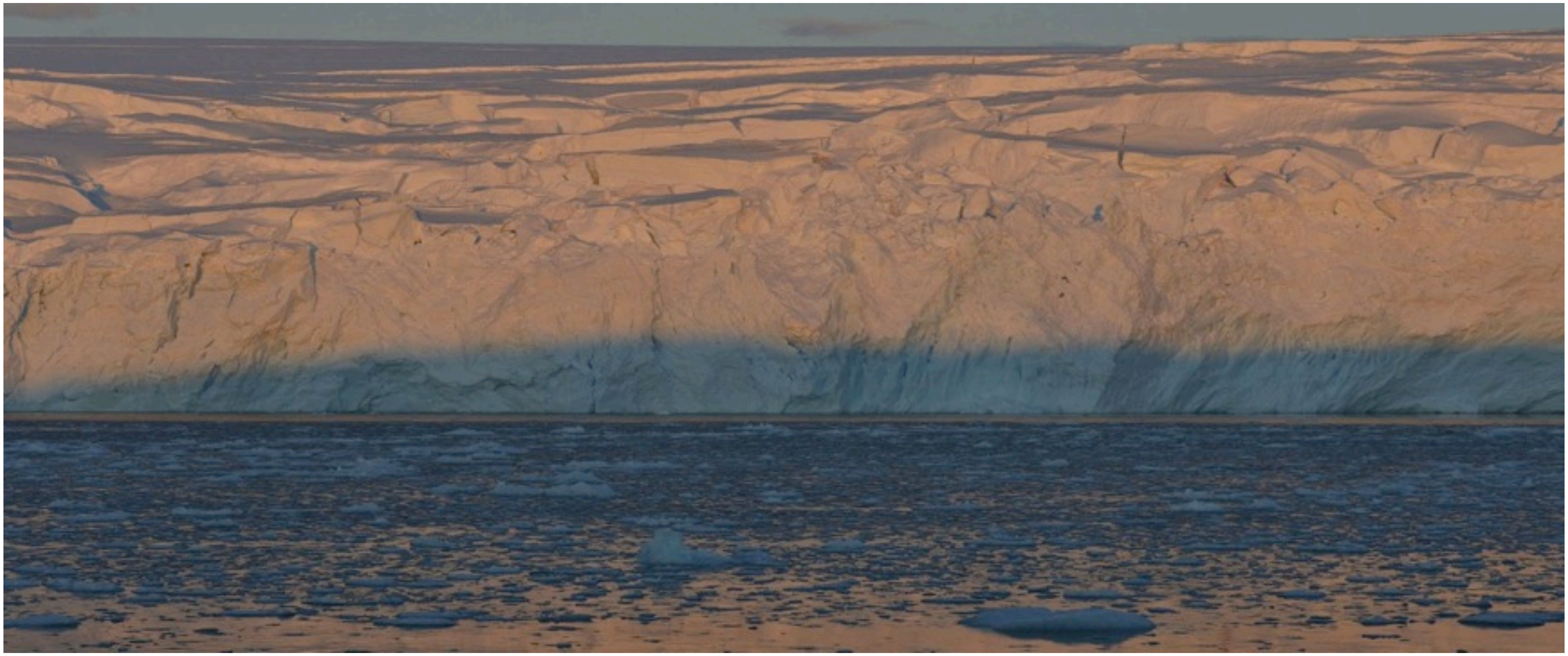

Joellen L. Russell
Associate Professor, Department of Geosciences
The University of Arizona

SOCCOM
Southern Ocean Carbon and Climate Observations and Modeling

GEOSCIENCES
University of Arizona

Collaborators:

Mike Winton, Ron Stouffer, Steve Griffies, John Dunne
John Krasting, Sergey Malyshev & Keith Dixon
at NOAA's Geophysical Fluid Dynamics Laboratory

Paul Goodman, Zachary Naiman, Jessica Rudd
at the University of Arizona, Dept. of Geosciences

What is the role of the Southern Ocean in the global climate system?

1. It may account for up to half of the annual oceanic uptake of anthropogenic carbon dioxide from the atmosphere (cf., Gruber et al., 2009)
2. Vertical exchange in the Southern Ocean is responsible for supplying nutrients that fertilize three-quarters of the biological production in the global ocean north of 30°S (Sarmiento et al., 2004)
3. It may account for up to 70 ± 30% of the excess heat that is transferred from the atmosphere into the ocean each year (see analysis of IPCC AR4 models)
4. Southern Ocean winds and buoyancy fluxes are the principal source of energy for driving the large scale deep meridional overturning circulation throughout the ocean (e.g., Toggweiler and Samuels, 1998; Marshall and Speer, 2012)

The global energy imbalance goes into the ocean

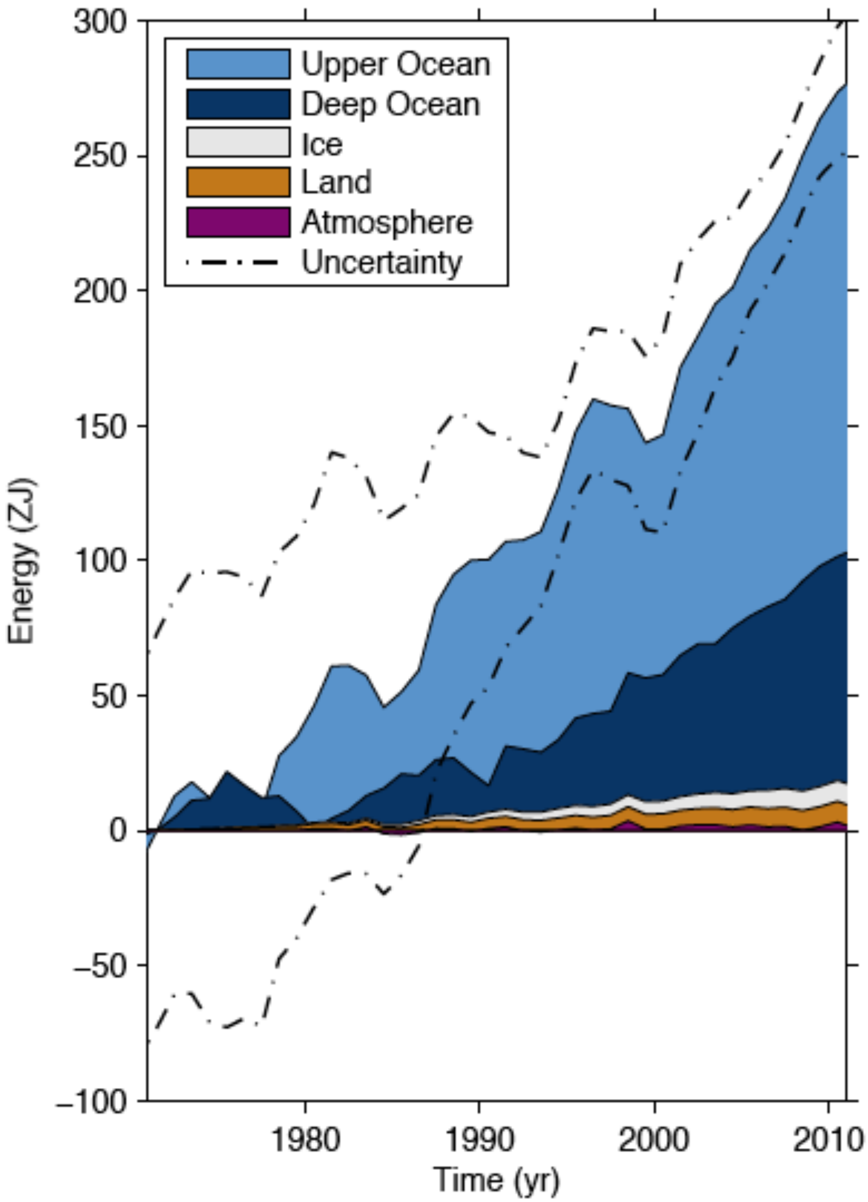

Box 3.1, Figure 1: Plot of energy accumulation within distinct components of Earth's climate system relative to 1971.

The Southern Ocean and the deep ocean are warming

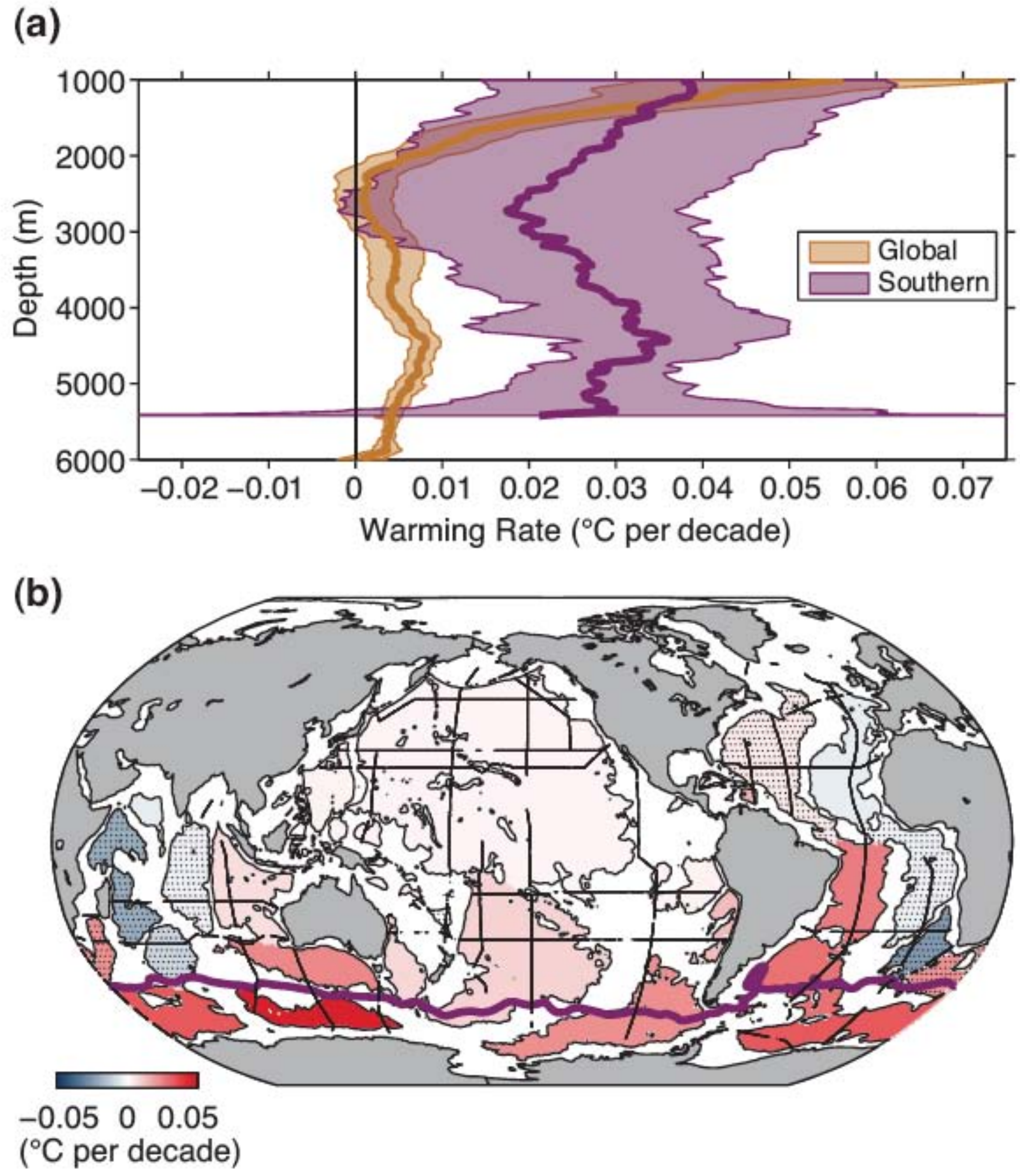

Warming Rate of Southern Ocean (purple) and global ocean (orange)

Figure 3.3: a) Areal mean warming rates (°C per decade) versus depth (thick lines) with 5 to 95% confidence limits (shading), both global (orange) and south of the Sub-Antarctic Front (purple), centred on 1992–2005. **b)** Mean warming rates (°C per decade) below 4000 m estimated for deep ocean basins (thin black outlines), centered on 1992–2005.

Warming Rate of deep ocean (>4000m)

Carbon Emissions Since 1950

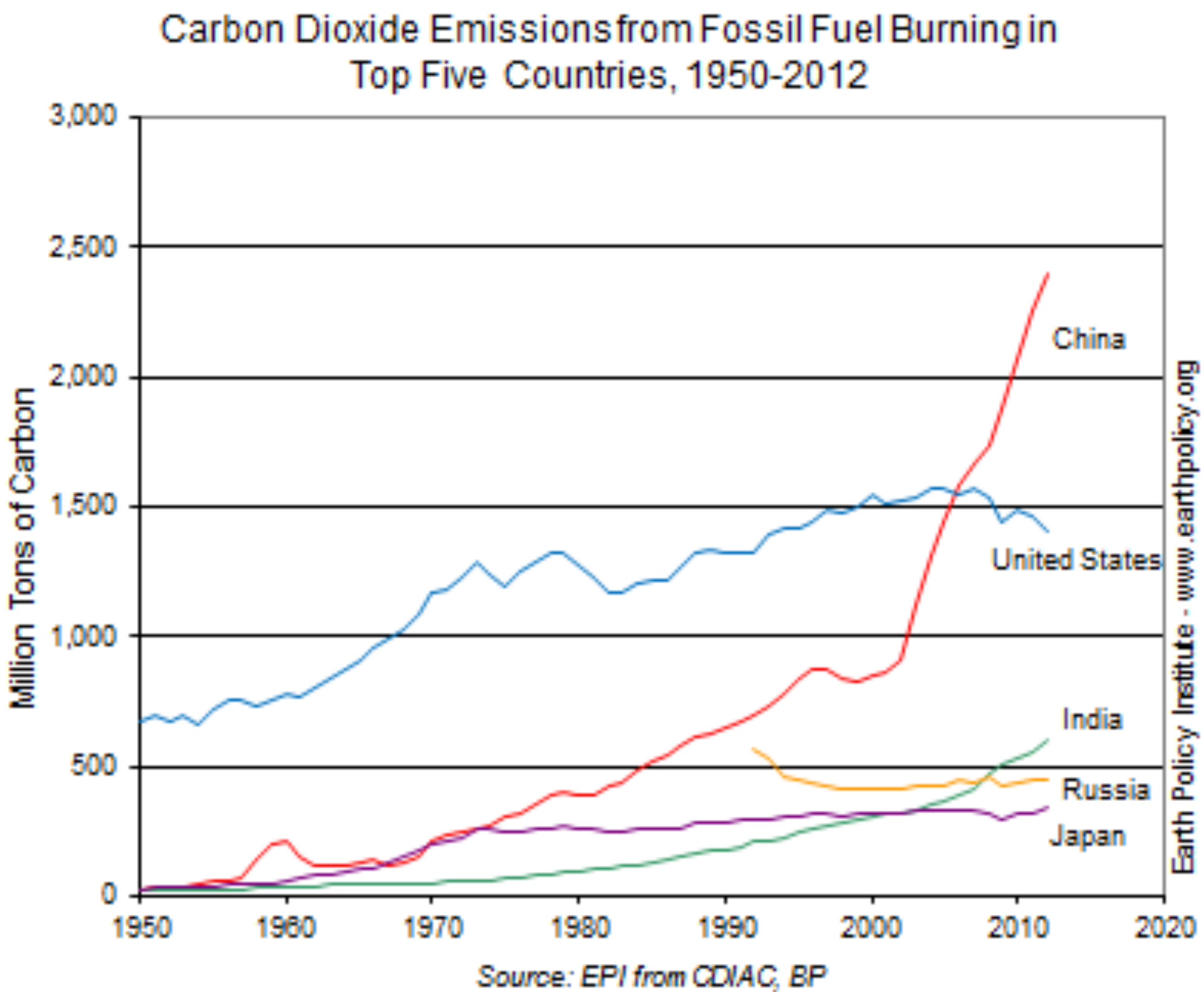

Although the U.S. Is responsible for more cumulative emissions since 1950, China is now the largest emitter of CO_2

Observed Stratospheric Temperature Trends

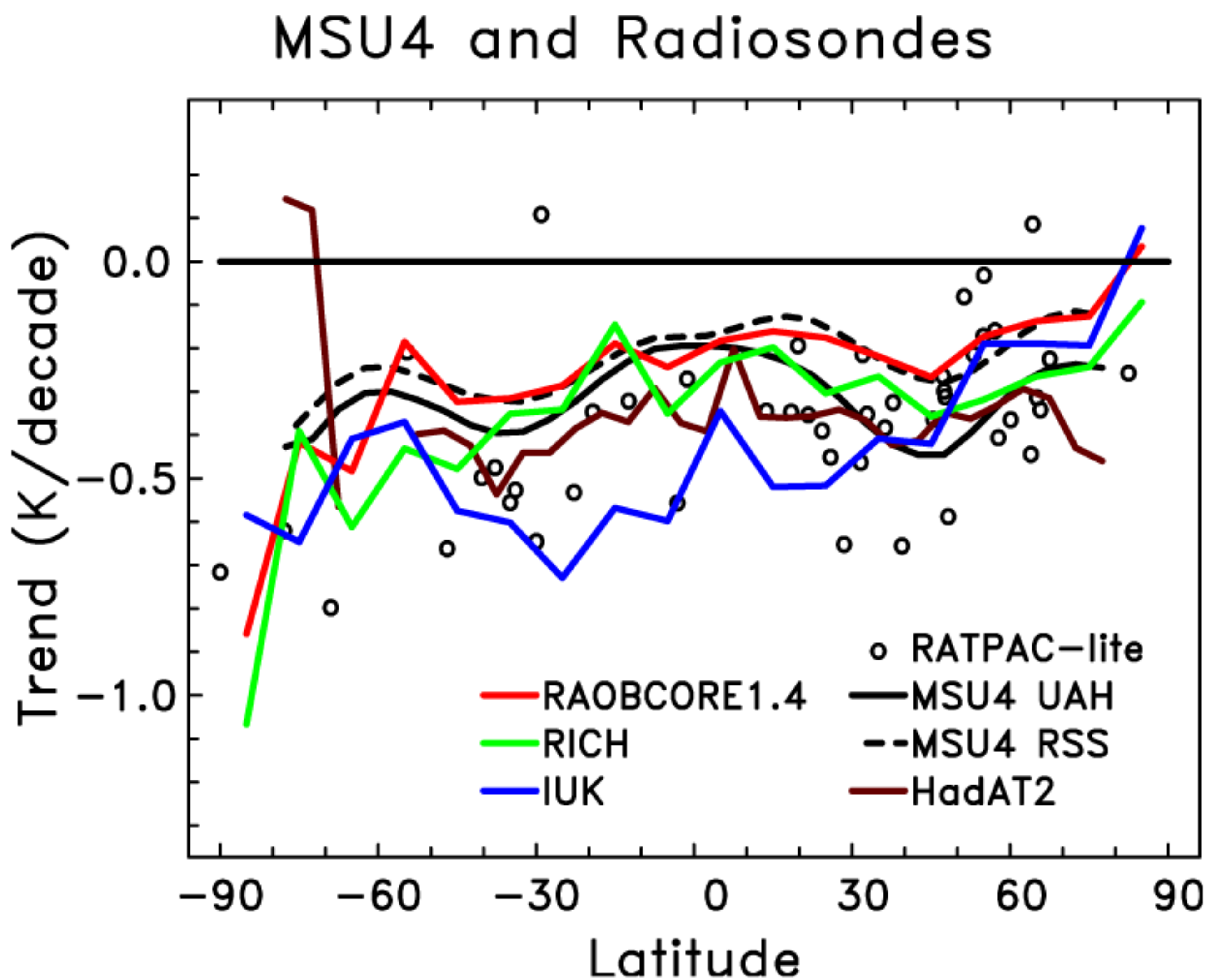

Turner et al., 2012

Attribution of Jet Forcing (Model Results)

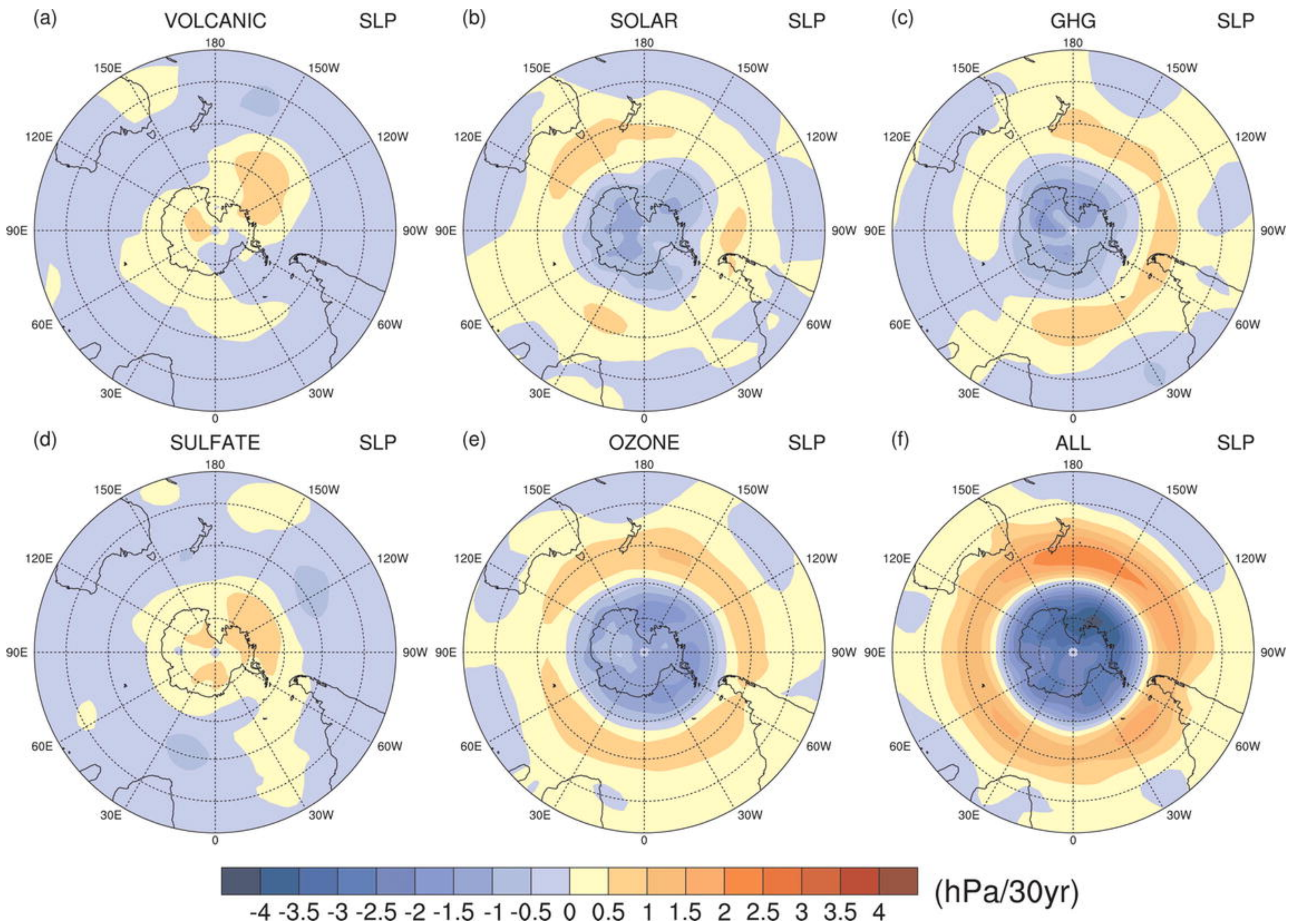

Arblaster & Meehl, 2006

Causes of the Poleward Shift of the SH Westerlies (Simulated)

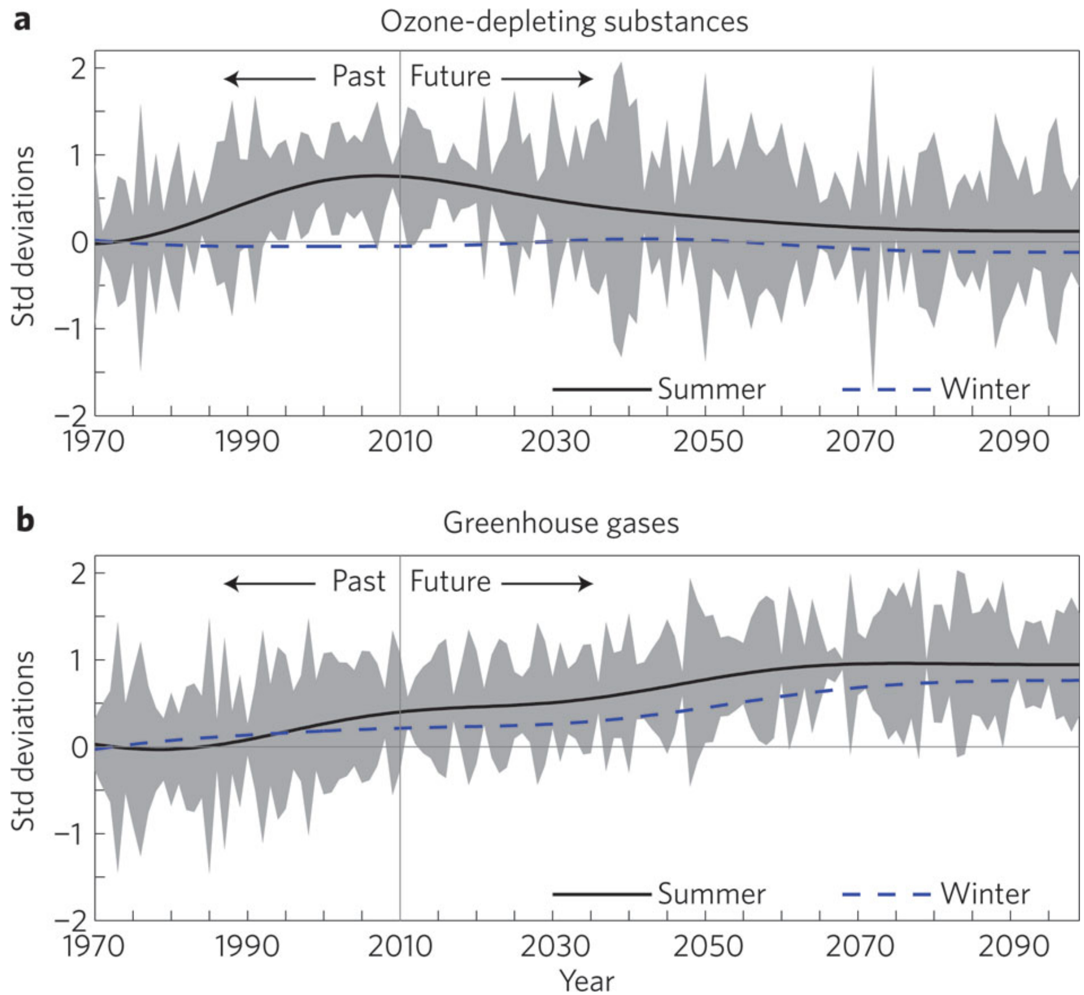

a) Forcing with ozone-depleting substances; b) forcing with greenhouse gases.

From Thompson et al., 2011

Winter Storm Track Changes

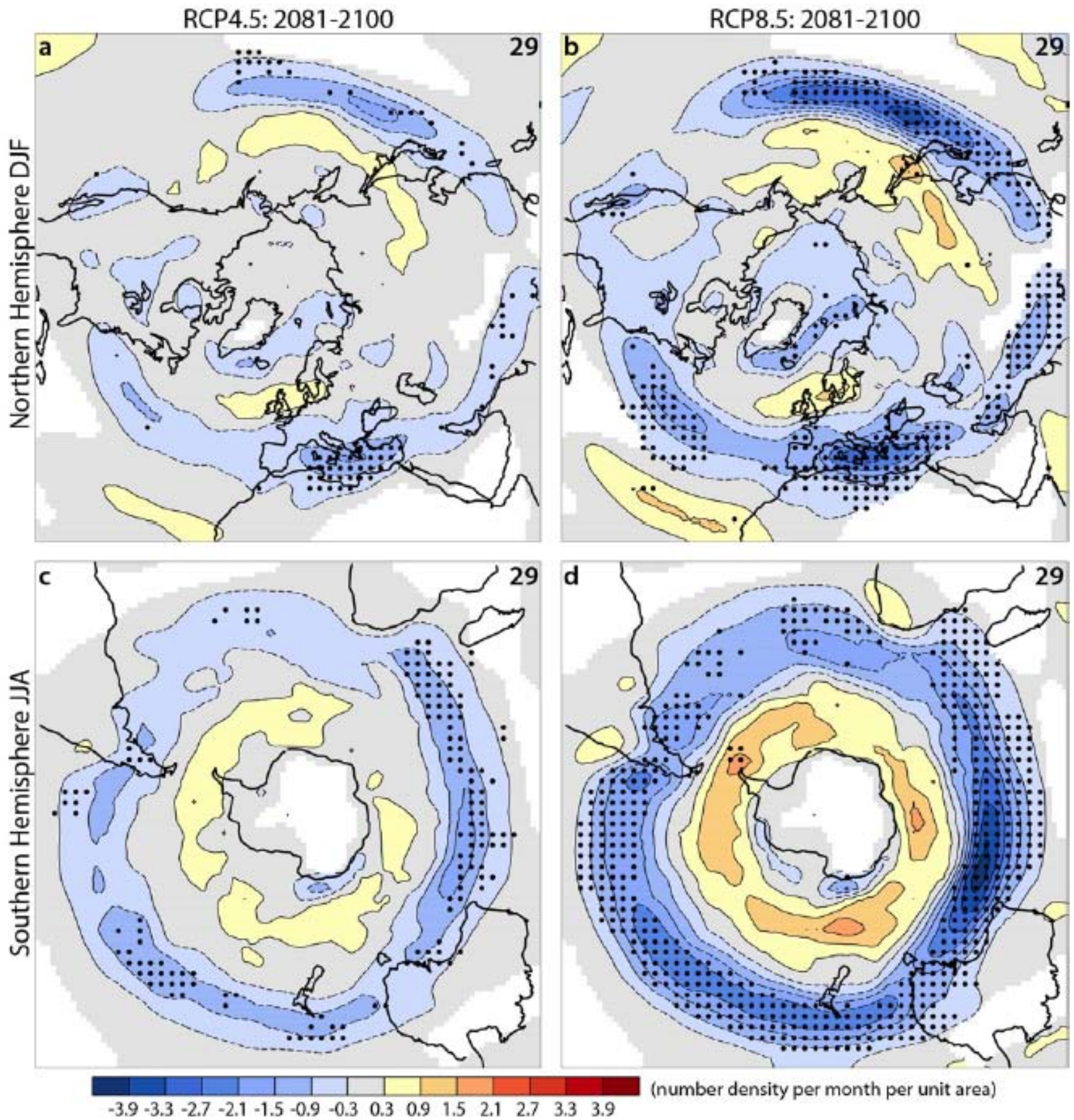

AR5 – Fig. 12.20

Simulations of the winds are getting better and are likely to continue their poleward shift over the near future.

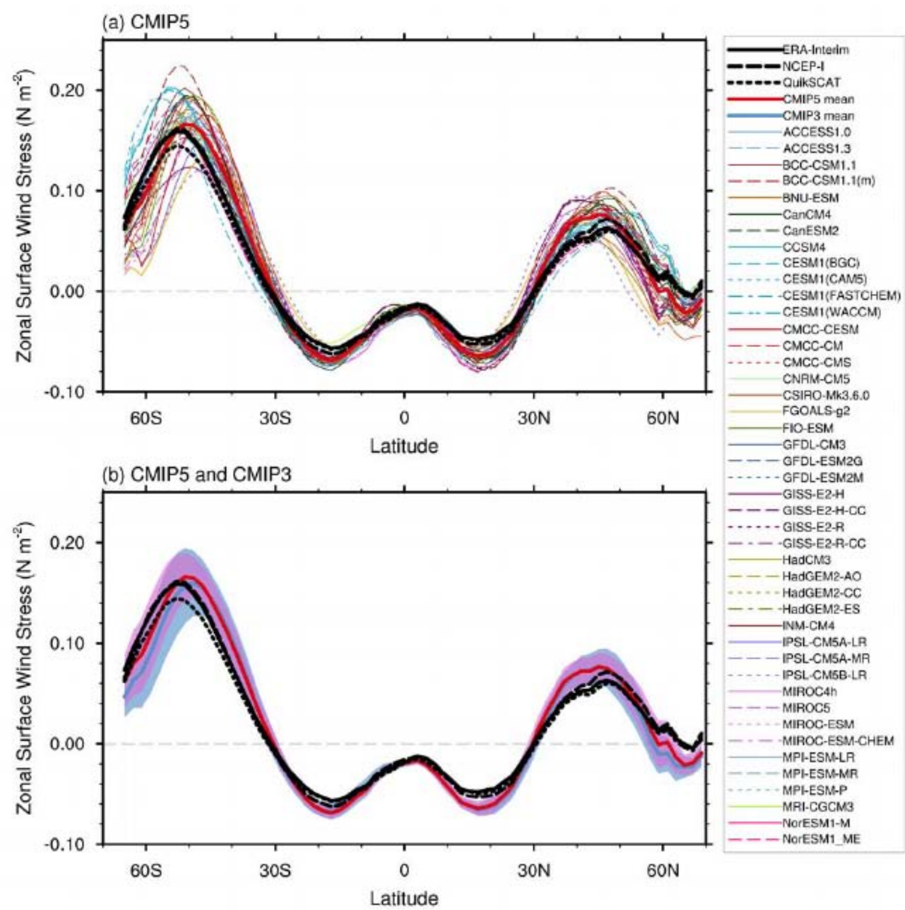

Figure 9.19: Zonal-mean zonal wind stress over the oceans in (a) CMIP5 models and (b) multi-model mean comparison with CMIP3.

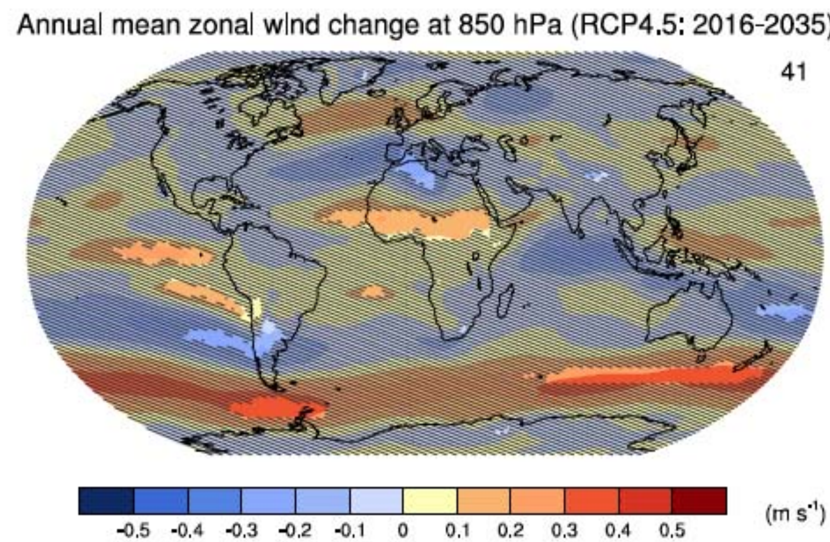

Figure 11.15: CMIP5 projected changes [m/s] in zonal (west-to-east) wind at 850hPa for 2016–2035 relative to 1986–2005 under RCP4.5.

"The equatorward shift of the westerlies in the southern ocean is slightly reduced in CMIP5 relative to CMIP3."

"The average 2016–2035 SH extra-tropical storm tracks and zonal winds are *likely* to shift poleward relative to 1986–2005."

Bracegirdle et al., 2013

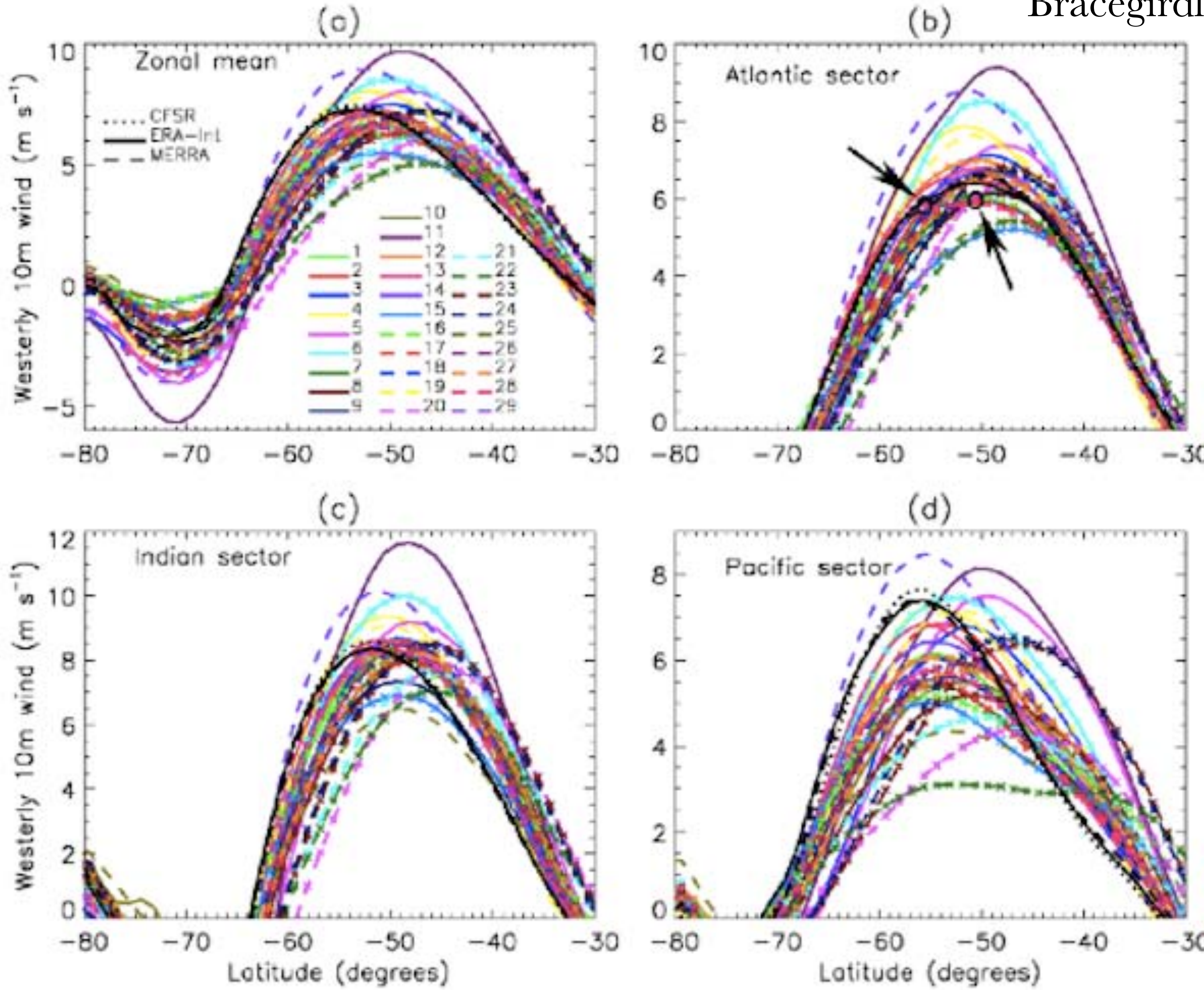

Figure 2. (a) Zonal mean annual mean 10 m westerly wind climatology for the period 1985–2004 as a function of latitude. (b), (c) and (d) show the same but for the Atlantic, Indian and Pacific sectors, respectively (note the different scales on the y axes). The colored solid and dashed lines indicate the CMIP5 models with overlaid star symbols indicating high-top models. The black solid, dotted and dashed lines show output from ERA-Interim, CFSR and MERRA, respectively. The arrows indicate double maxima exhibited by model 28 (MRI-CGCM3).

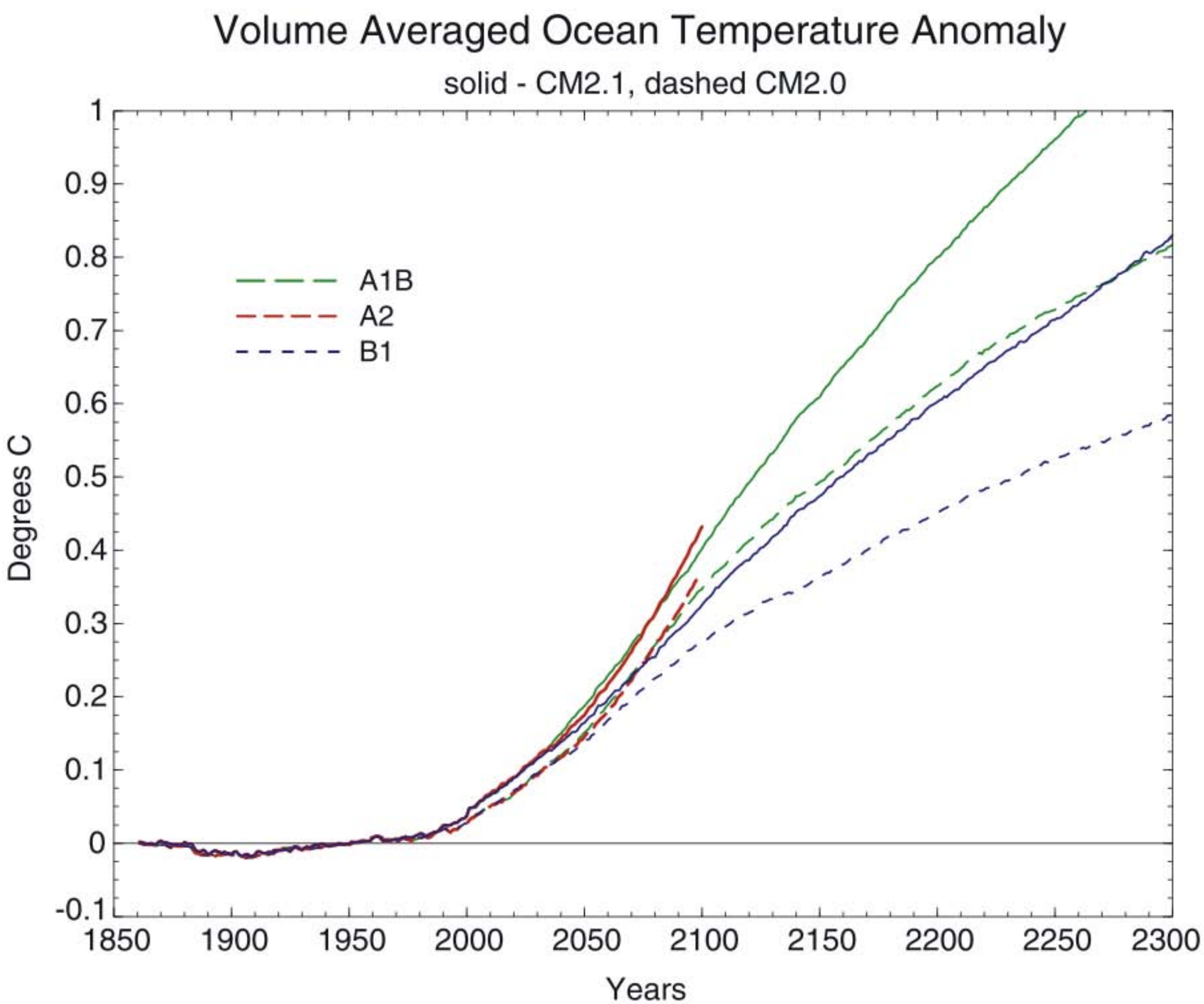

Time series of volume averaged ocean temperature difference (°C) for the various integrations minus the control.

CM2.1 results are indicated by solid lines, CM2.0 by dashed lines.

The line color indicates the type of integration:
historical – blue,
A2 – red,
A1B – green,
B1 – blue

Stouffer et al., 2006

Surface Zonal Wind Stress (N/m^2, Annual Mean)

SOSE

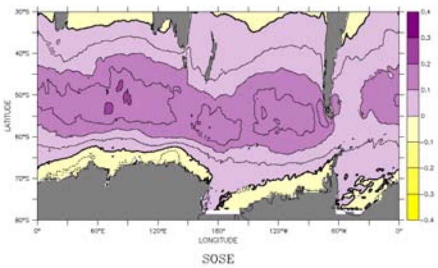

CMCC

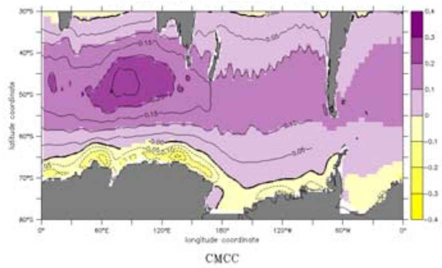

CNRM

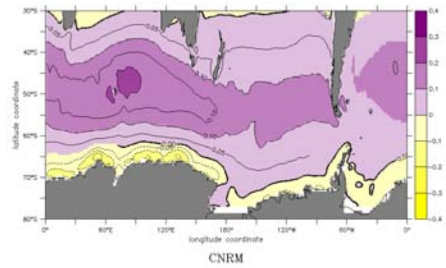

CSIRO

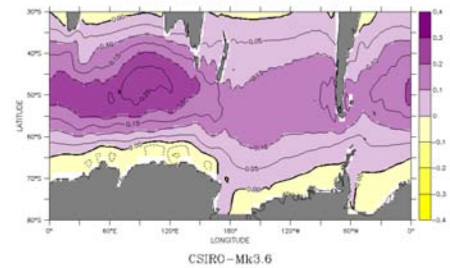

ESM2G

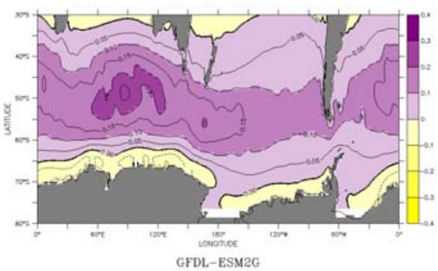

ESM2M

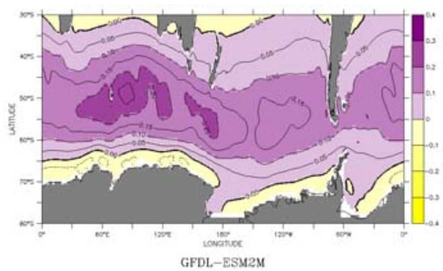

IPSL-MR

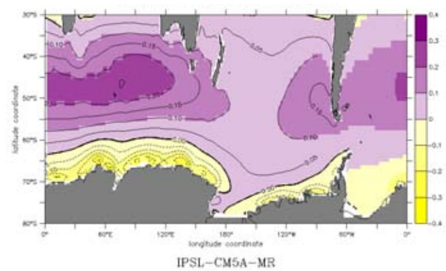

IPSL-LR

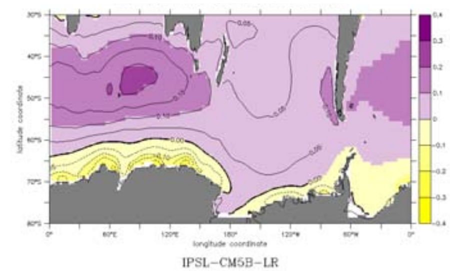

MIROC

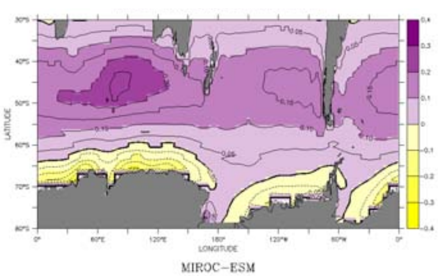

MPI-MR

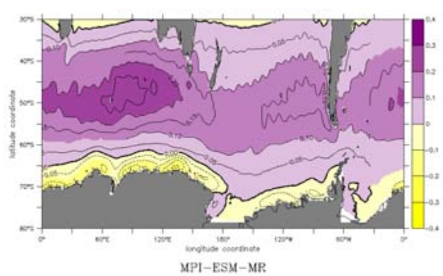

MRI

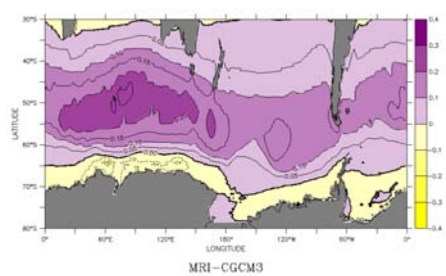

NorESM

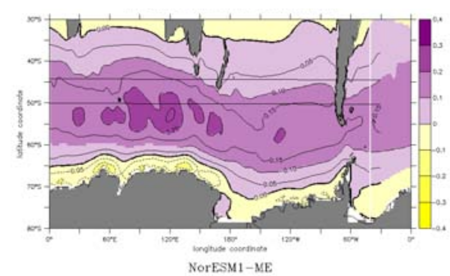

All averages are for model years 1986-2005, SOSE is annual average for 2008

Sea Surface Height

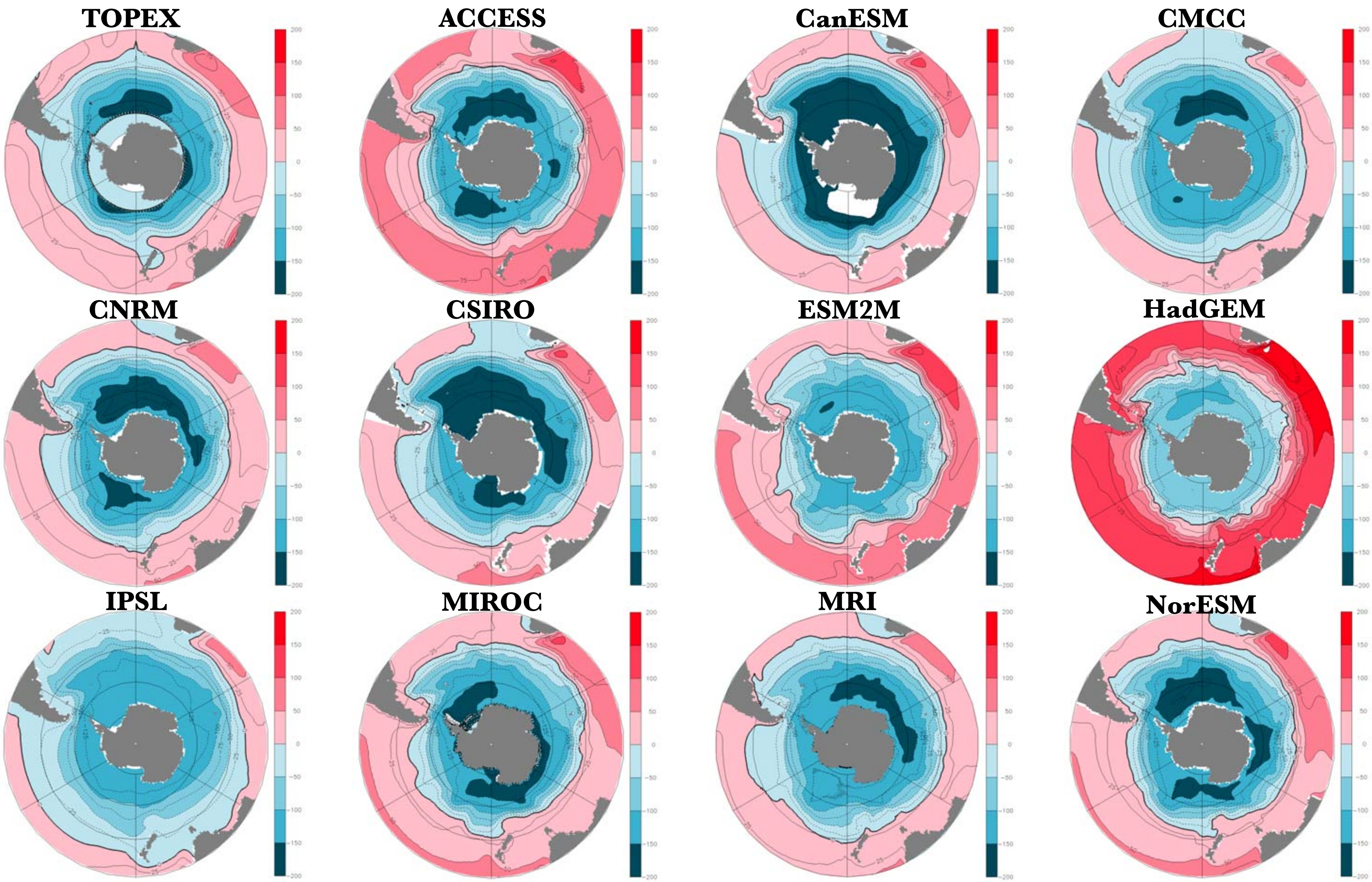

Free-surface elevation (in cm) from the observations (TOPEX; Fu et al. 1994) and the CMIP5 ocean simulations.

Drake Passage Transport: Zonal Velocity at 69°W

- Annual mean, 2001-2005
  Zonal Velocity
  Values are net transport
  through Drake Passage

SOSE (2008) 148.1 Sv | GFDL-ESM2M 133.7 Sv | BCC-CSM2 156.6 Sv | CSIRO-Mk3.6 108.2 Sv

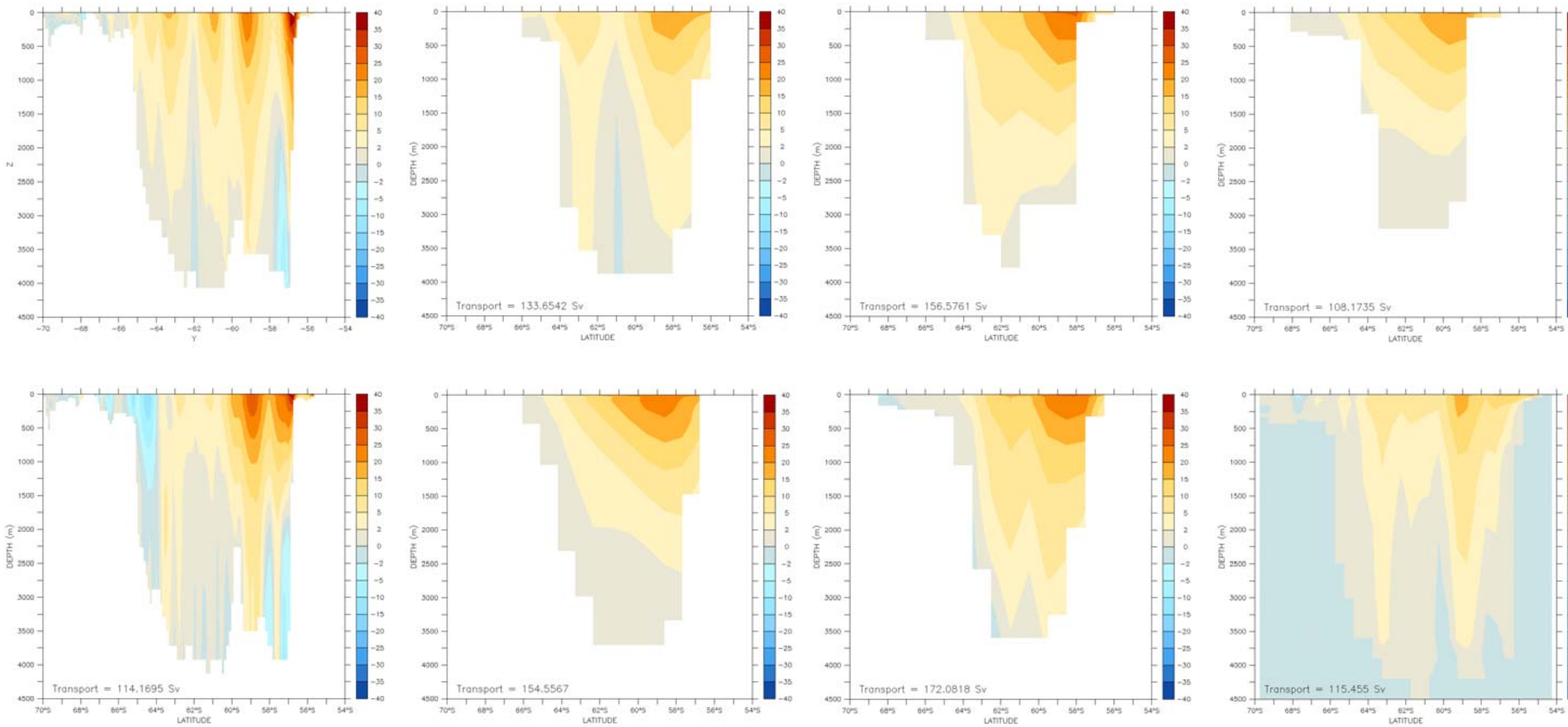

GFDL-CM2.5 114.2 Sv | CanESM2 154.6 Sv | HadGEM2-ES 172.1 Sv | MRI 115.5 Sv

Frontal structure is not captured by lower resolution models

Sea Ice Extent (Maximum/Minimum)

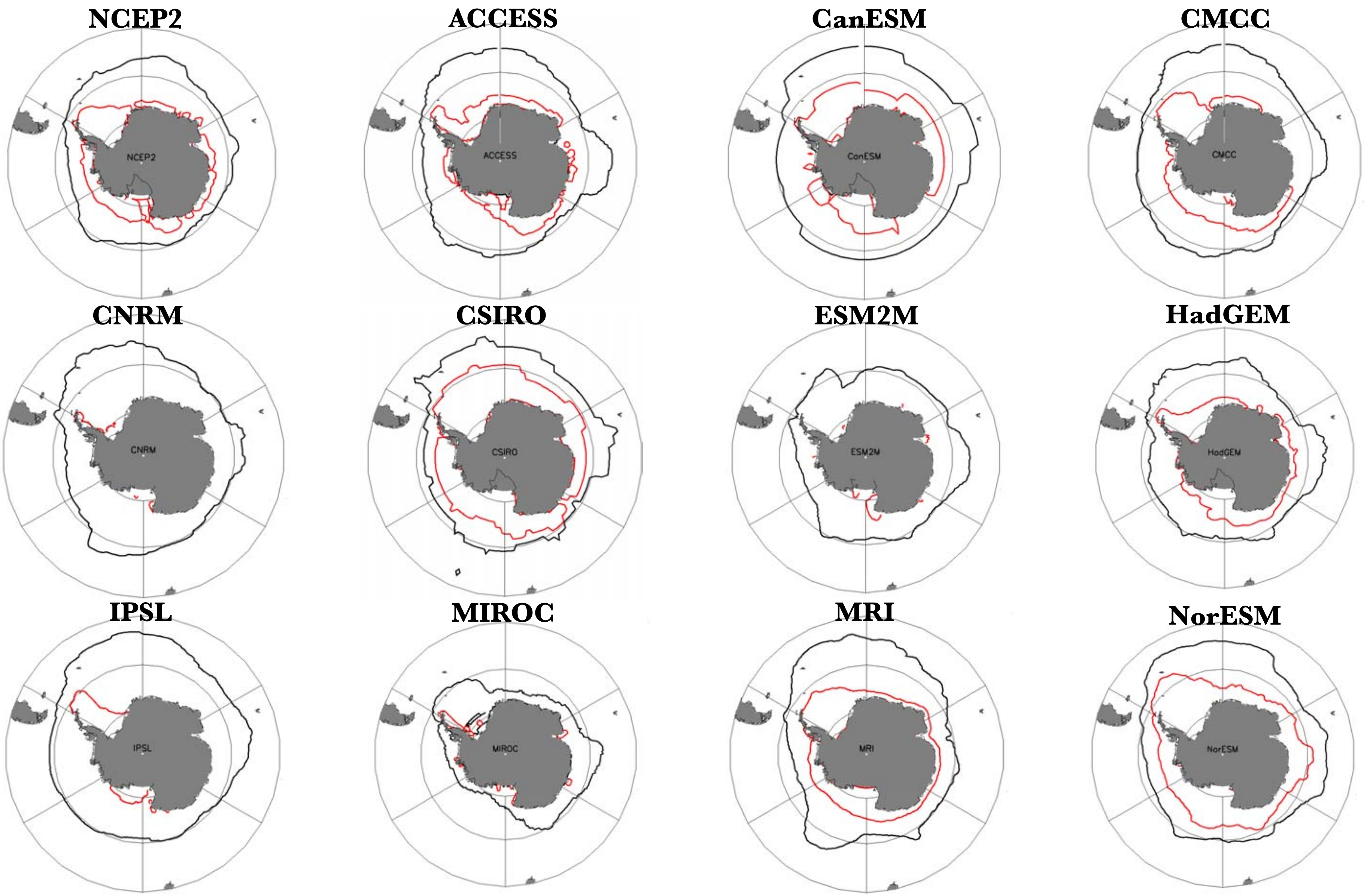

Annual maximum (black) and minimum (red) extent of sea ice – defined as the 15% ice coverage contour.

Temperature Error at 30°W (Atlantic)

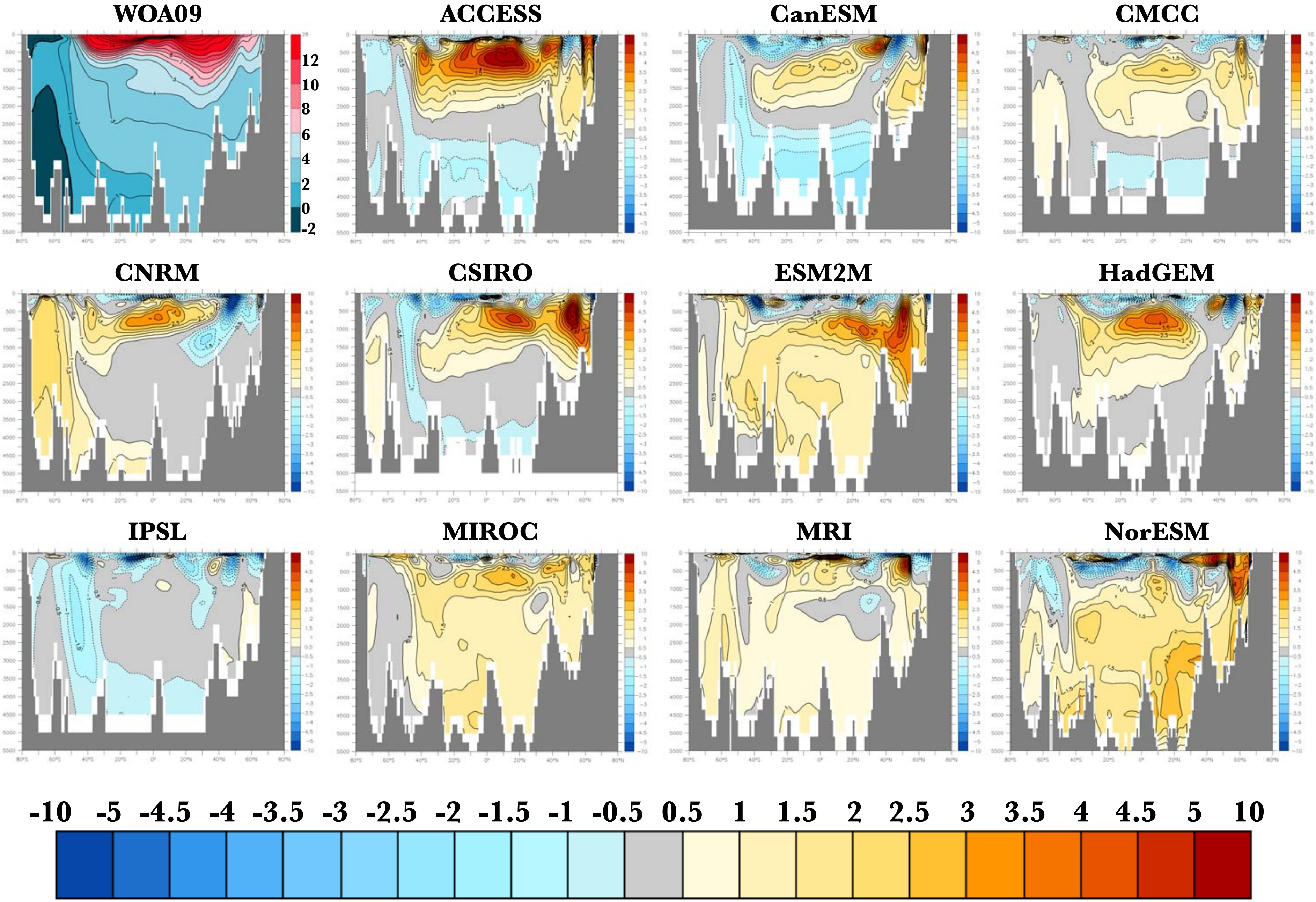

Salinity Error at 30°W (Atlantic)

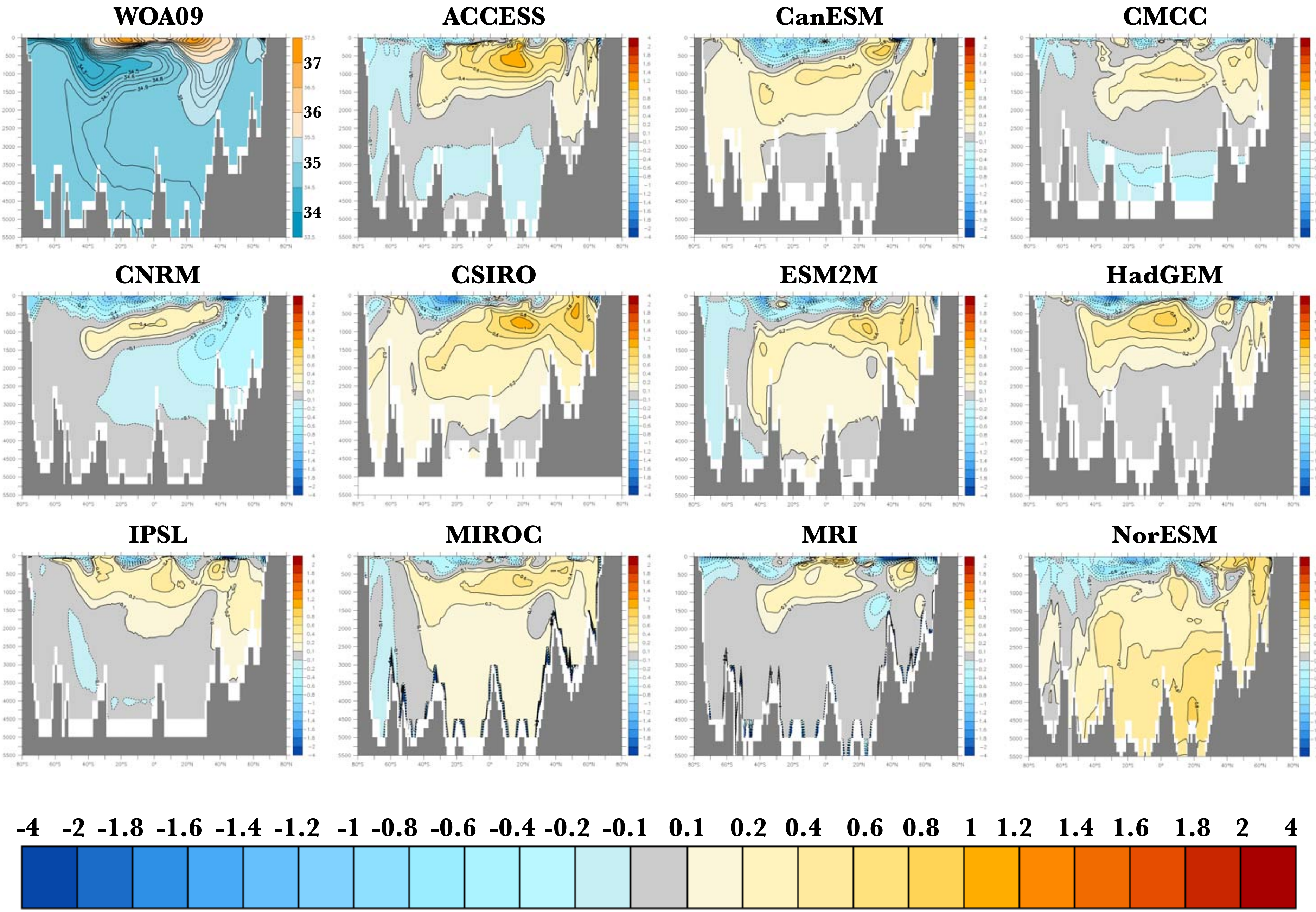

ACC (Sv) vs Maximum Wind Stress (N/m^2)

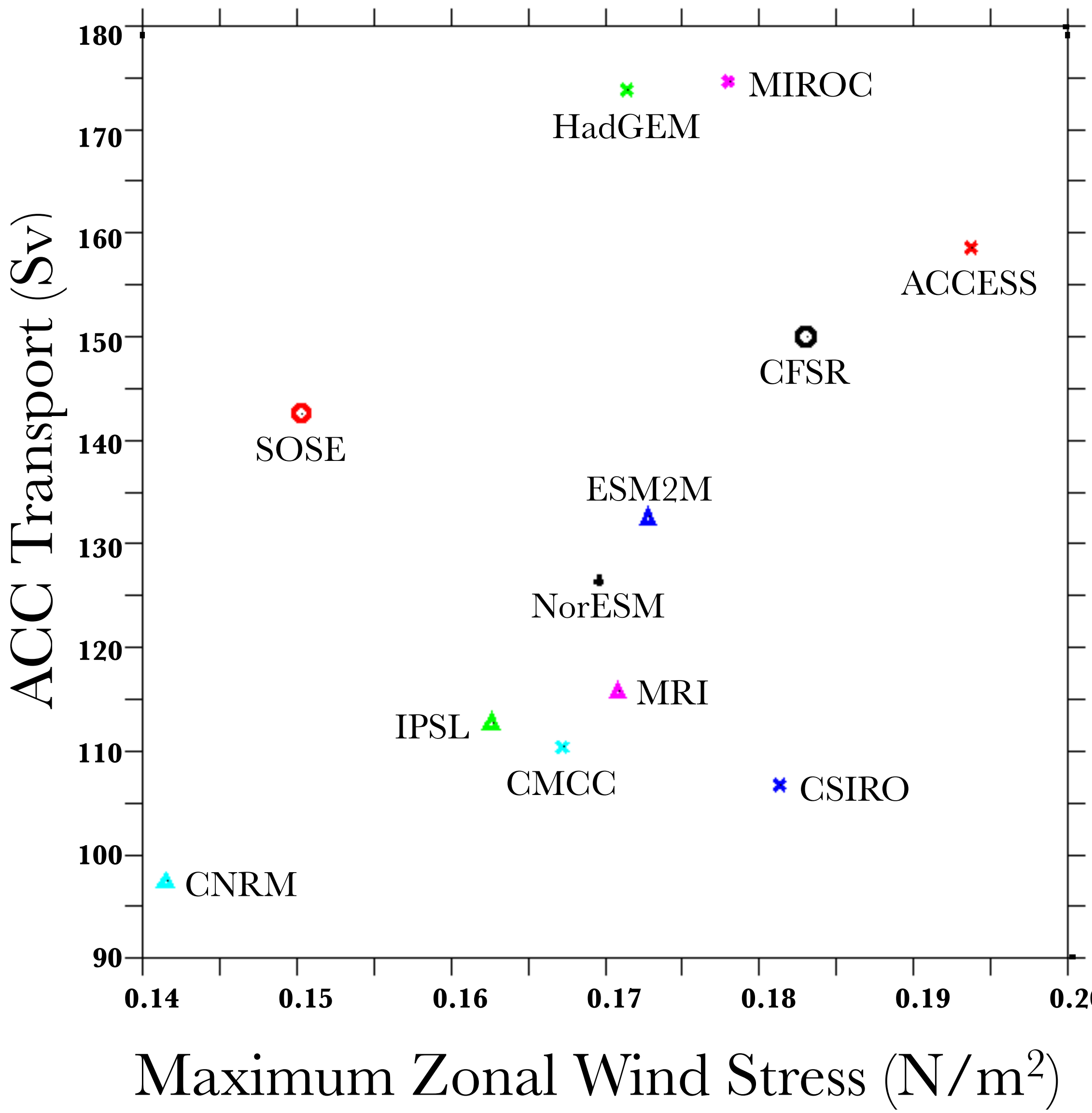

Scatter plot of ACC transport at Drake Passage against the maximum zonally-averaged wind stress.

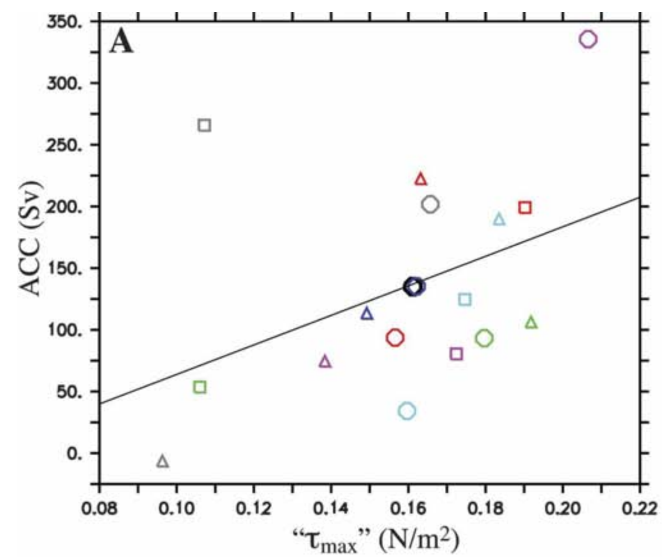

ACC (Sv) vs Latitude of Maximum Wind Stress (°S)

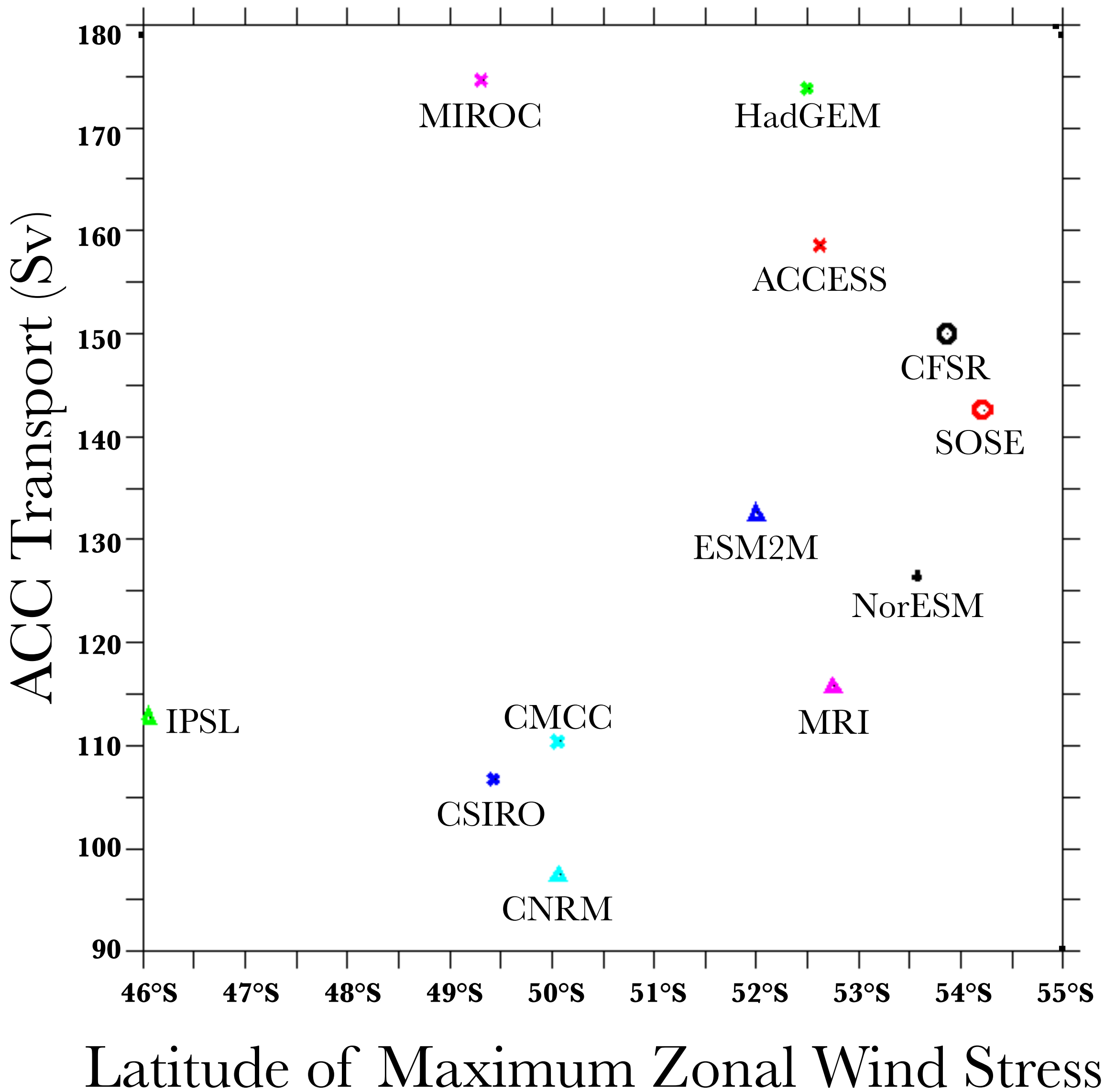

Scatter plot of ACC transport at Drake Passage against the the latitude of the maximum zonally-averaged wind stress.

High Resolution Model Development

Scientific Goals:

- **Developing improved models (higher resolution, improved physics, reduced bias) for studies of variability and predictability on intra-seasonal to decadal time scales**
- **Explore impact of atmosphere and ocean on climate variability and change using a high resolution coupled model**
- **New global coupled models: CM2.4, CM2.5, CM2.6**

	Ocean	Atmos	Computer	Status
CM2.1	100 Km	250 Km	GFDL	Running
CM2.3	100 Km	100 Km	GFDL	Running
CM2.4	10-25 Km	100 Km	GFDL	Running
CM2.5	10-25 Km	50 Km	DOE/GFDL	Running
CM2.6	4-10 Km	50 Km	DOE/GFDL	Running

Zonal Wind Stress (N/m^2, GFDL Only)

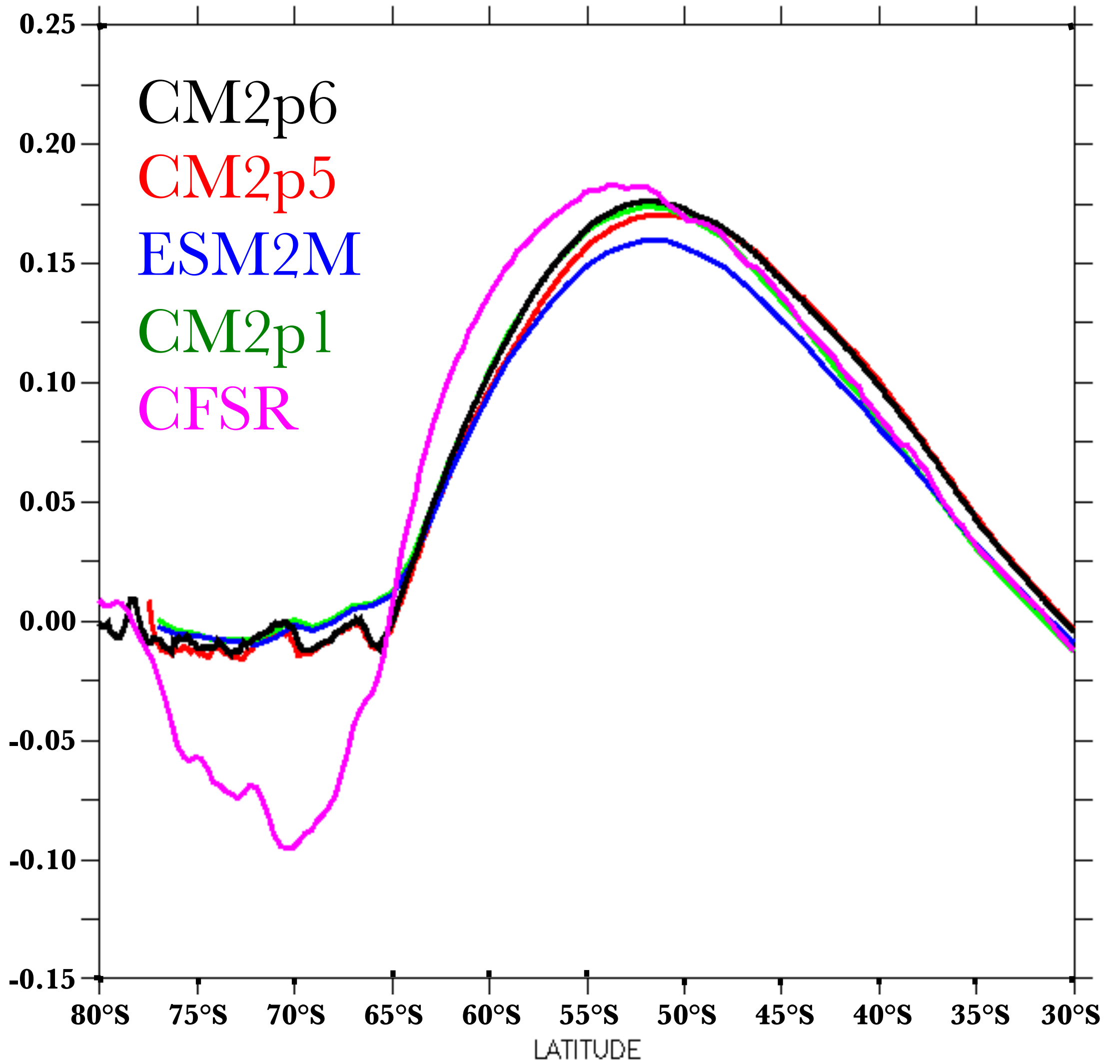

Averaged over the 20-year period prior to the start of the 1% to 2x CO2 run

Note that all of the models are still slightly weaker and equatorward-shifted from the observations (CFSR).

CMIP3 – SresA1B for GFDL-CM2.1 (black) and GFDL-CM2.0 (red)

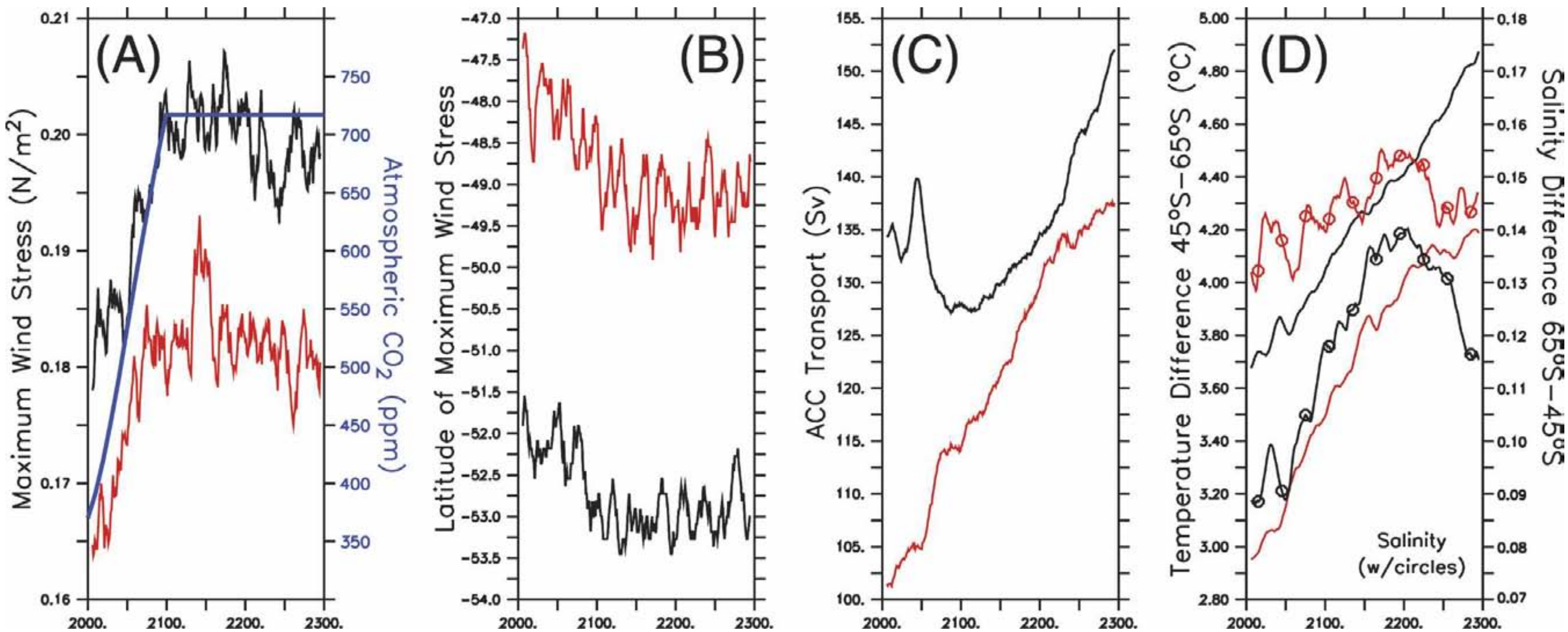

Time series of (a) the maximum zonally averaged wind stress between 70° and 30°S, (b) the latitude of the maximum zonally averaged wind stress, (c) the strength of the ACC transport at Drake Passage, and (d) the mean temperature (solid) and salinity (solid with circles) differences (averaged globally from the surface to 2500-m depth) between 65° and 45°S. In (a)–(d), the black line is the result from the CM2.1 experiment and the red line is the result from the CM2.0 experiment. The blue line in (a) is the time history of atmospheric CO2 used to force both model runs. An 11-yr centered running mean filter has been applied to each of the curves.

(Russell et al. 2006b)

CMIP3 – SresA1B for GFDL-CM2.1 (black) and GFDL-CM2.0 (red)

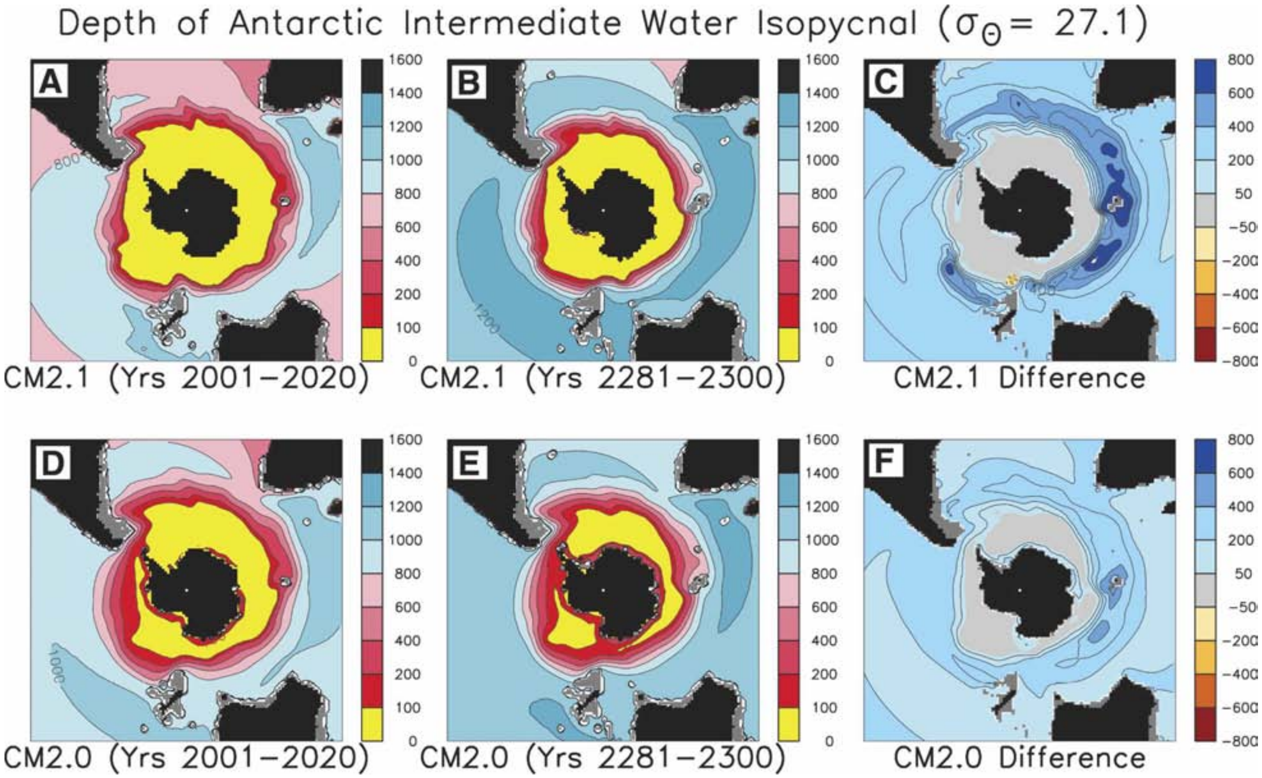

CM2.6 at end of 1% run

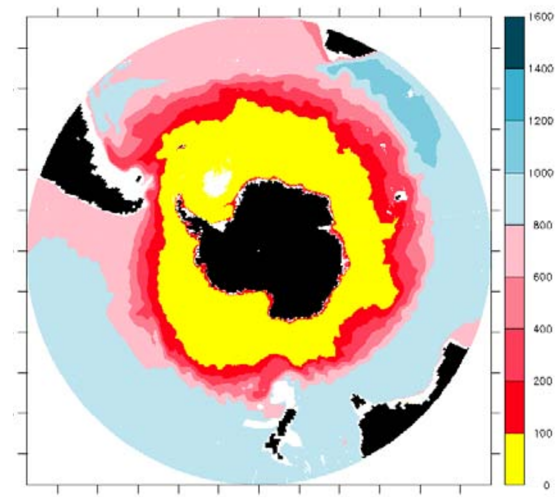

Depth of the σ_θ = 27.1 isopycnal surface (meters), the conventional proxy for AAIW (Talley 2003), at (a) the start of the CM2.1 experiment; (b) the end of the CM2.1 experiment; (d) the start of the CM2.0 experiment; and (e) at the end of the CM2.0 experiment. Those areas where the isopycnal outcrops or is less than 100 m deep are shaded in yellow. Those areas in which the water column is less dense than 27.1 are shaded in dark gray. Also shown are the change in depth of the AAIW isopycnal (in meters) for (c) the CM2.1 experiment and (f) the CM2.0 experiment. Dark gray regions in (c) and (f) are locations where the water column is less dense than 27.1 at all depths at all times.

(Russell et al. 2006b)

Area of the AAIW Outcrop & Volume of "Young" Water (old)

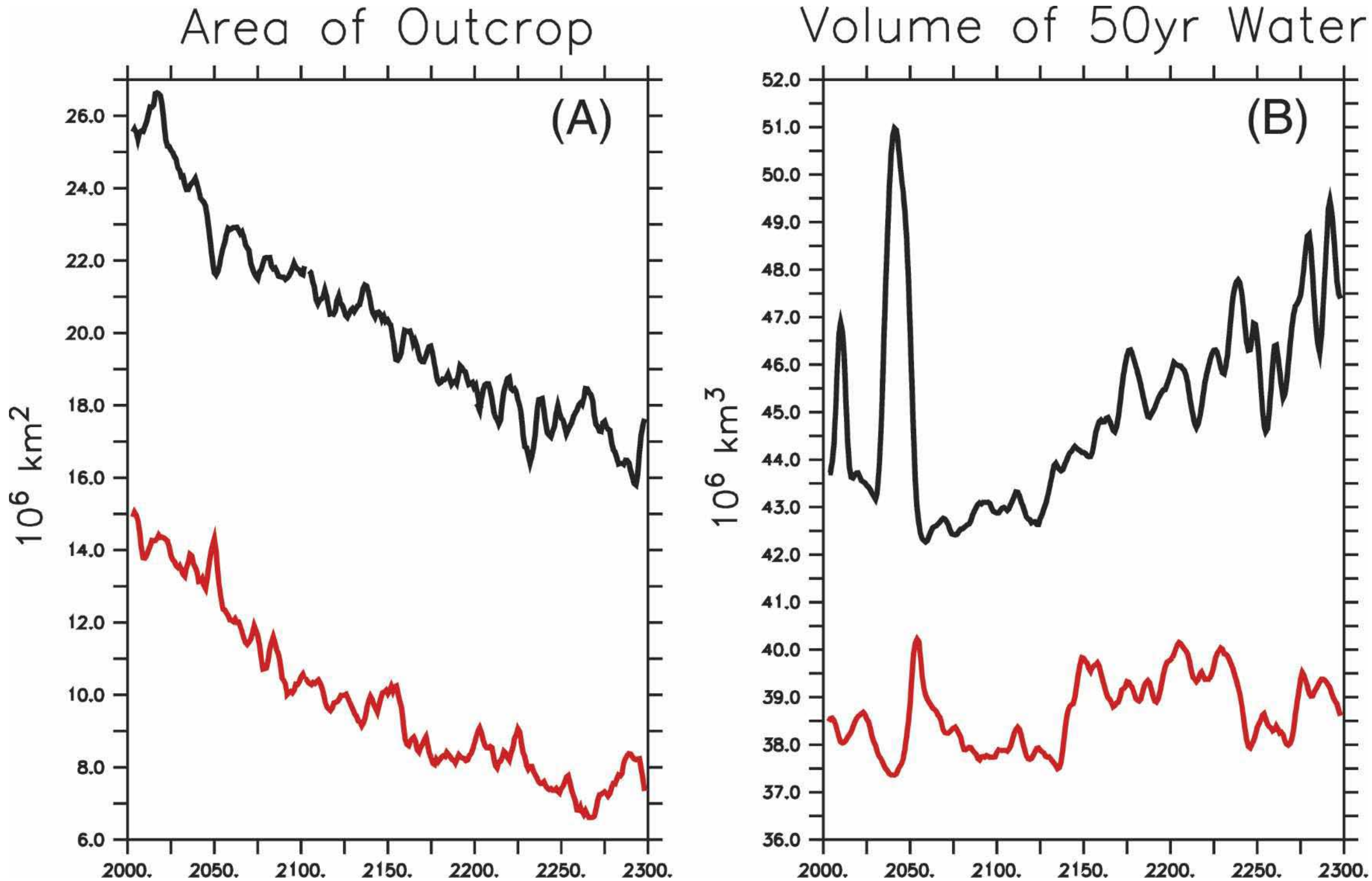

The integrated outcrop area (the yellow regions in Fig. 2) over the course of the SRES A1B scenario for CM2.1 (black) and CM2.0 (red). (b) The integrated volume of water younger than 50 yr (south of 30°S) over the same period of time.

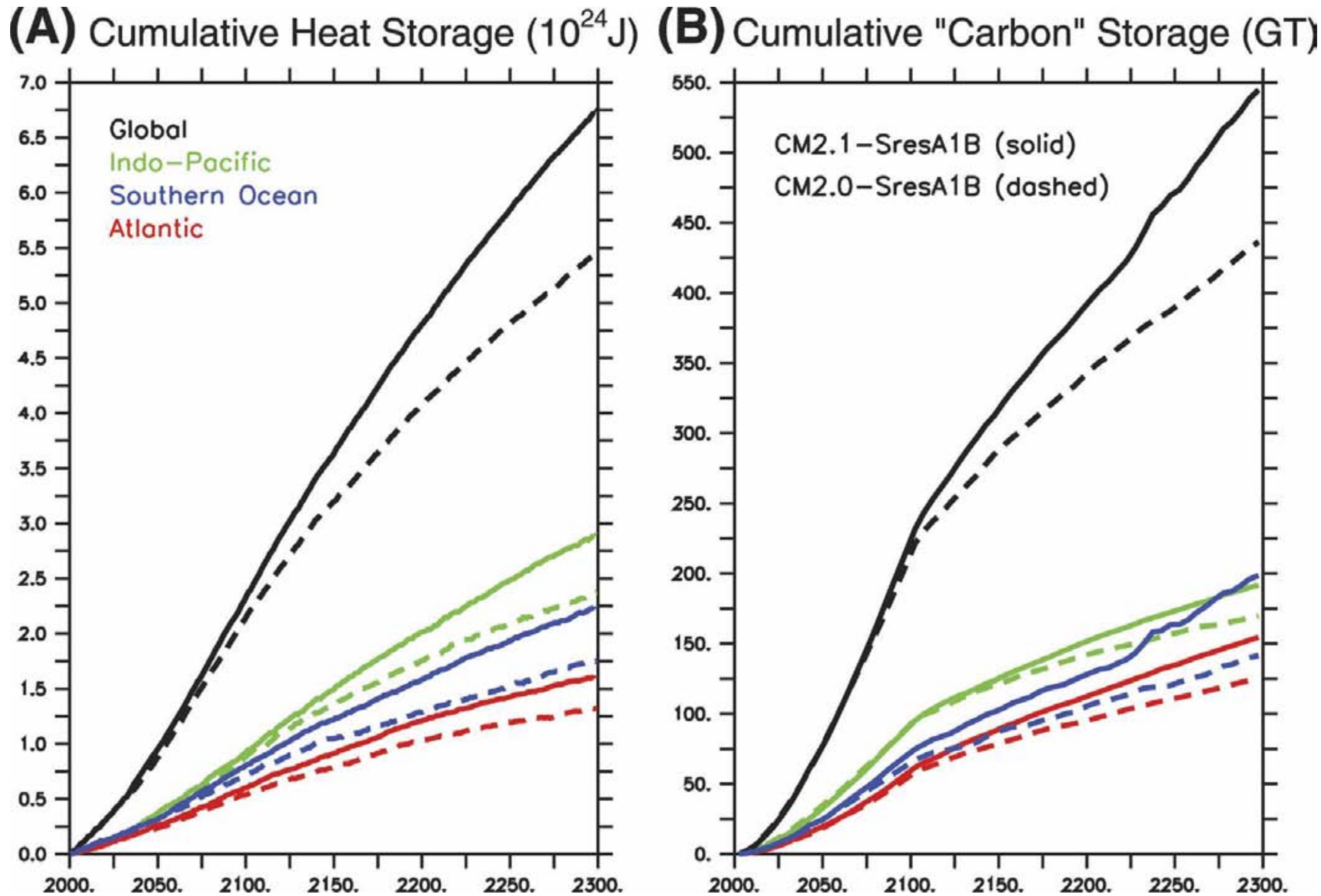

The cumulative uptake of (a) heat and (b) carbon for the CM2.1 (solid) and CM2.0 (dashed) SresA1B scenarios over the global ocean (90°S–90°N, 0°–0°; black), the Southern Ocean (90°–30°S, 0°–0°; blue), the Indo-Pacific Ocean (30°S–90°N, 20°E–80°W; green), and the Atlantic Ocean (30°S–90°N, 80°W–20°E; red).

Conclusions:

We need to reduce the uncertainty in our projections of the Southern Ocean's role in climate.

1) We need more in situ biogeochemical observations of the Southern Ocean, including floats, ships, moorings, etc.

2) We need more Southern Ocean Climate Process Teams

3) We need more Observationally-based climate model metrics

4) We need a Southern Ocean model intercomparison project